Electronic Supplementary Material (ESI) for Analyst.

Supplementary Information

Surface Dependent Enhancement in Water Vapor Permeation through Nanochannels

*Kaushik K. Rangharajan, Prashanth Mohanasundaram, A.T. Conlisk, Shaurya Prakash**

Department of Mechanical and Aerospace Engineering, The Ohio State University, Columbus, OH 43210, USA

*Corresponding author: Shaurya Prakash, prakash.31@osu.edu

Table of Contents

S1. Analysis for capillary driven flow inside surface modified nanochannel

The change in dynamics of the liquid (water) meniscus when it encounters an abrupt transition from a hydrophilic to hydrophobic surface during capillary filling (see Figure 1c, main manuscript) inside the nanochannel is discussed here. The relationship between the net distance l, covered by the moving meniscus in time t for a slit-like nanochannel of height h, with a rectangular cross-section is given by the Lucas-Washburn equation, [S1]

$$l = \sqrt{\frac{h\,\sigma_{lv}\,t\cos\theta}{3\mu}} \tag{S1}$$

Where, σ_{lv} is the liquid-air surface tension, θ is the equilibrium contact angle, and μ is the bulk liquid viscosity.[S1-S5] Past studies demonstrate that capillary filling in hydrophilic silica nanochannels with height varying from 27 – 150 nm agree with equation S1, wherein a linear relationship is obtained between the filling length l and square root of time ($t^{0.5}$).[S1-S5] However, the impact on capillary filling rate when the meniscus encounters an abrupt transition from a hydrophilic to hydrophobic surface inside a nanochannel remains unknown. Specifically, the role of a hydrophobic surface in either instantaneously halting a progressing meniscus against gradual flow deceleration remains uninvestigated.

Fig. S1 depicts the filling length of the water meniscus inside all the three nanochannels connecting the draw and feed microchannels, plotted as a function of ($t^{0.5}$) to compare against the Lucas-Washburn equation.[S2-S5] In agreement with the Lucas-Washburn equation (equation S1) and past experimental results in silica nanochannels,[S2-S5] Fig. S1 shows a linear slope (1000 μm/s$^{0.5}$) between filling length l and $t^{0.5}$ for un-modified bare silica nanochannels. A similar linear slope of 930 μm/s$^{0.5}$ is observed in FTS-modified nanochannels up to a filling length of ~890 μm ($t^{0.5}$ = 1.18 s$^{0.5}$), and subsequently, the slope gradually decreases to 675 μm/s$^{0.5}$ between $t^{0.5}$ = 1.2 and 1.29 s$^{0.5}$. From Fig. S1, a further decrease in value of average slope to 212 μm/s$^{0.5}$ between $t^{0.5}$ = 1.35 and 1.41 s$^{0.5}$ was observed before the meniscus halted (as verified visually with more details on integrity of the vapor trap in the main manuscript) at a distance of 96 μm from the draw microchannel (Fig. 1c, main manuscript).

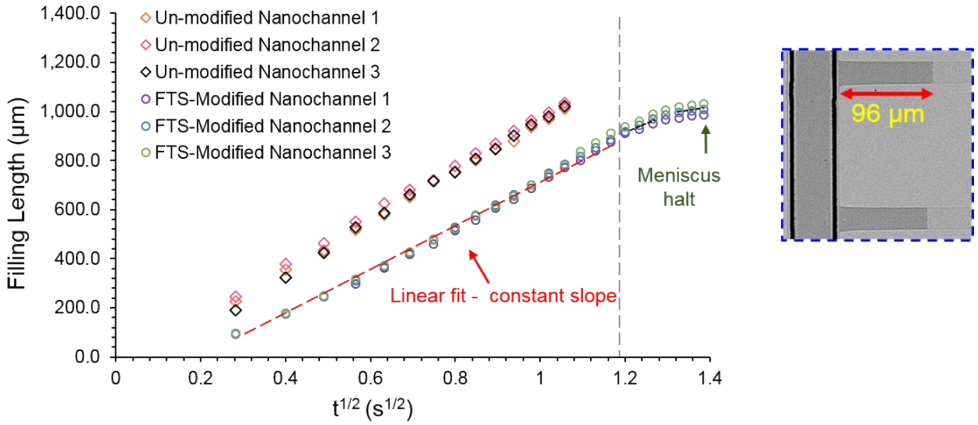

Figure S1: Capillary filling length l, plotted as a function of square root of time ($t^{0.5}$). Capillary filling dynamics of meniscus in un-modified nanochannels is in agreement with Lucas-Washburn equations along the entire filling length. In contrast, a constant slope is observed for capillary filling in FTS-modified channels up to a filling length of 890 µm ($t^{0.5}$ = 1.18 $s^{0.5}$), and subsequently, the slope gradually decreases to 675 µm/$s^{0.5}$ between $t^{0.5}$ = 1.2 and 1.29 $s^{0.5}$ before halting completely at a distance of 96 µm from draw (inset).

The rate of capillary filling of water meniscus through partially FTS-modified nanochannel was recorded (Fig. 1c, main manuscript) and compared against capillary filling in un-modified silica devices. Over a capillary filling length of 1013 µm inside the nanochannel, the filling velocity was estimated experimentally by dividing the average distance traveled by the meniscus inside the three nanochannels for each time interval (80 ms). Theoretically, the relationship between the capillary filling velocity and the filling length *l*, can be obtained by taking a derivative on both sides of Lucas-Washburn equation (equation S1),

$$2l\,dl = \frac{h\,\sigma_{lv}\cos\theta}{3\mu}dt$$
$$\frac{dl}{dt} = \frac{h\,\sigma_{lv}\cos\theta}{6\mu\,l} \qquad \text{(S2)}$$

Equation S2 depicts that an inversely proportional relationship exists between the expected capillary filling velocity and capillary filling length traversed by the meniscus. Fig. S2a shows the theoretically predicted velocity from equation S2 compared against the experimentally obtained capillary filling velocity in FTS-modified and un-modified nanochannels. Theoretical prediction for capillary filling velocity was observed to fall within experimental uncertainty for unmodified nanochannels for the entirety of filling length of 1013 µm. However, in the FTS-modified nanochannels with the vapor trap, the velocity estimate from equation S2 over-predicts the measured velocity near ~890 µm, which also corresponds to the location where a change in slope

was observed (Fig. S1). The capillary filling velocity also reduced from 453 ± 37 µm/s at capillary filling length of 890 ± 17 µm to 0 µm/s when the meniscus reaches a capillary filling length of 1013 µm. Therefore, over a distance of 123 ± 17 µm, prior to the physical location of the partial hydrophobic region constituting the vapor trap, the flow gradually decelerates.

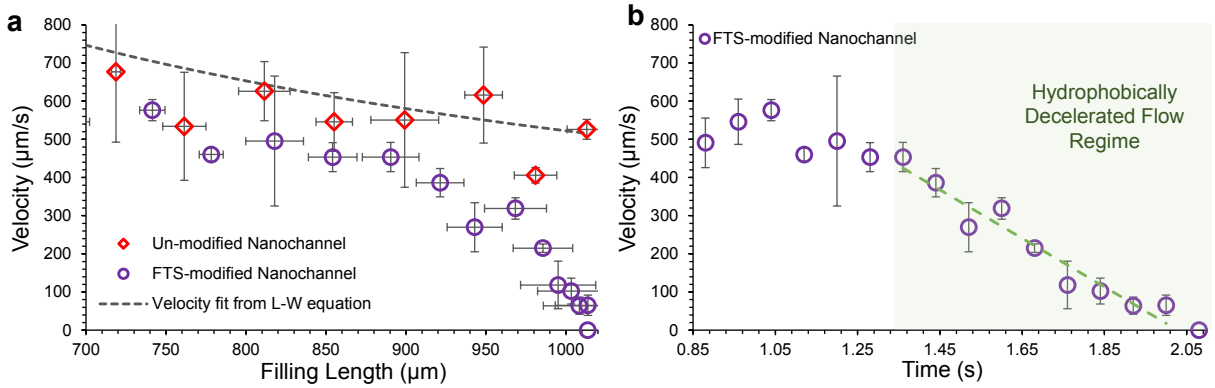

Figure S2: **(a)** *Measured capillary velocity in nanochannels as a function of filling length compared against theoretical velocity fit from equation S2 indicates capillary filling velocity for FTS-modified nanochannels is slower than the theoretical prediction as the flow approaches the vapor trap.* **(b)** *Plot of capillary filling velocity as a function of time shows a linear reduction in velocity beyond 1.36 s, indicating the meniscus is subjected to a constant deceleration while approaching the vapor trap. Error bars represent ± standard deviation (s.d) in the mean arising from multiple measurements (n = 3).*

S2. Electrical conductance measurements across the vapor trap

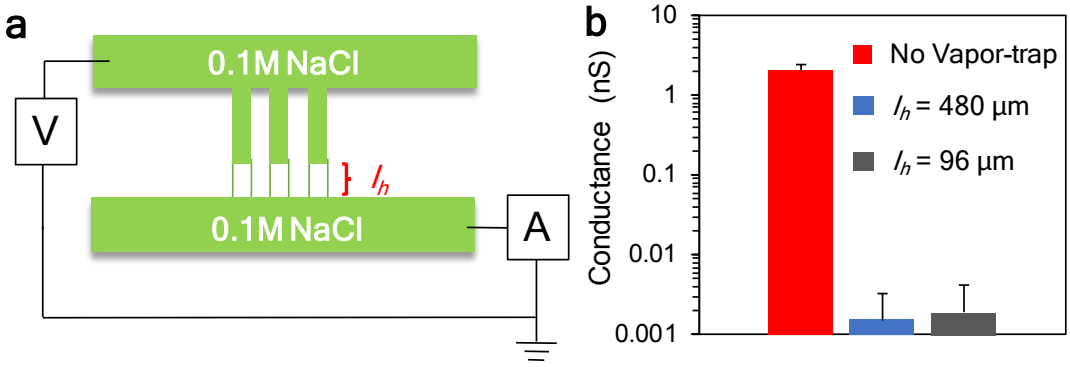

Figure S3: ***(a)*** *Feed and draw reservoirs were filled with 0.1 M NaCl solution. Keithley 3390 function generator was used to apply a potential difference between the two microchannels. Current was recorded using a Keithley 6485 picoammeter to estimate nanochannel conductance using methods reported previously.*[S6] ***(b)*** *In comparison to devices with no vapor-traps, conductance of devices with a hydrophobic length l_h = 96 µm, 480 µm were lower by about three orders of magnitude. The significantly lower conductance across the vapor trap confirms the visual observation that there is no liquid providing a conduction path across the vapor trap.*

S3. Calibration of Rhodamine B intensity for varying NaCl draw concentration

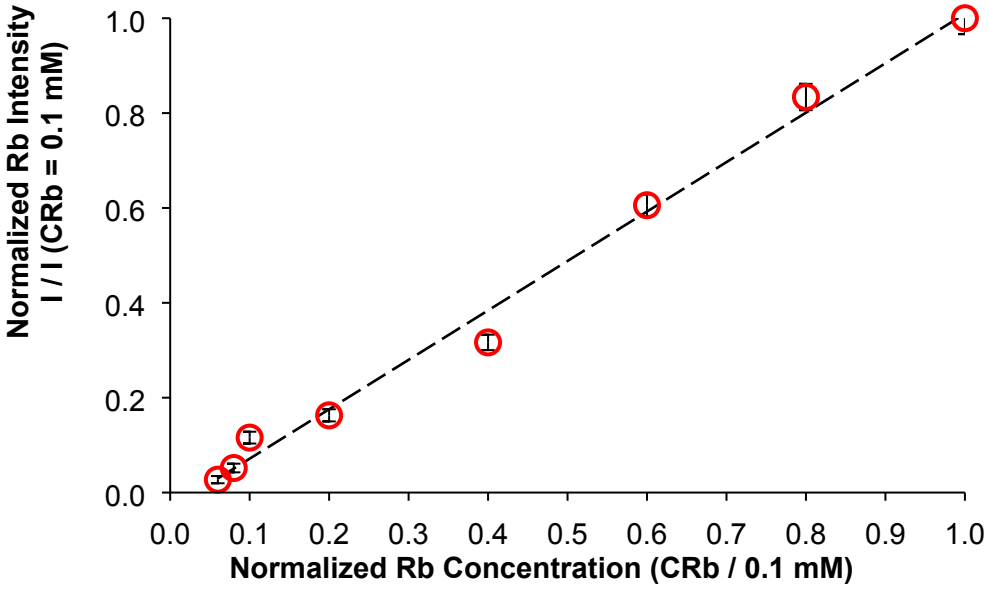

Figure S4: Calibration curve of Rhodamine B (Rb) dye mixed with sodium chloride (NaCl) electrolyte. Calibration was performed by filling microchannel with (6 µM Rb, 0.06 M NaCl) initially and gradually replacing the dilute dye with increasing dye/ salt concentration mixtures, all the way to 0.1 mM Rb, 1 M NaCl. A linear increase in dye intensity was observed with increase in Rb and NaCl concentration.

S4. Representative parameters used in the Unified Slip Model (1 M NaCL draw, DI water feed)

Vapor pressure of DI water – 3.17 kPa [S7]

Vapor pressure of 1M NaCl – 3.06 kPa [S7]

ΔP_{vap} = 0.11 kPa.

ξ (ratio of feed to draw vapor pressure) = 1.03

ρ_{wv} = 0.023 kg/m^3

μ_{wv} = 9.8 x 10^{-6} Pa·s [S8]

h = 80 nm.

$\overline{\alpha}$ = 2 [S9]

b = -1 [S9]

S5. Sensitivity Analysis on Unified slip model: Derivative of flux with TMAC, *α*, *b*

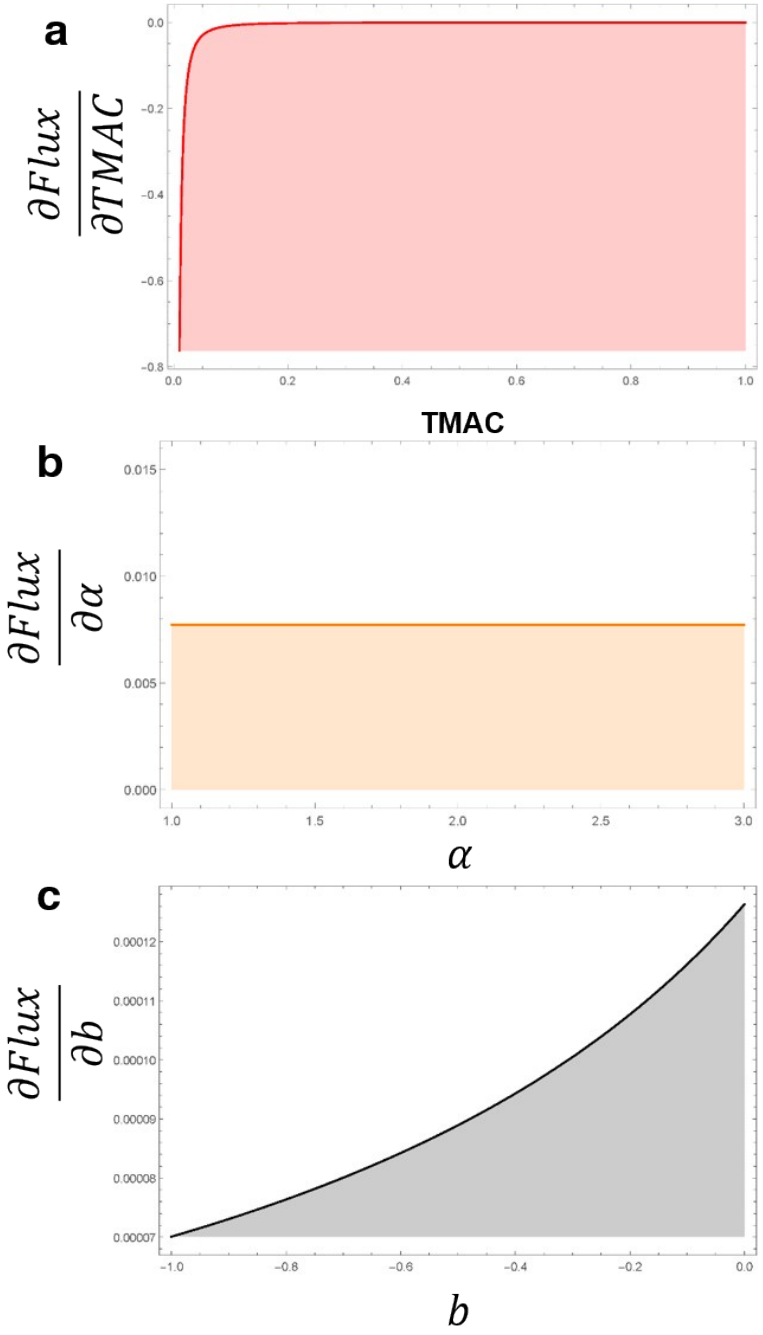

Figure S5: Sensitivity analysis of the rate of change of flux with the parameters employed in the unified slip model (Equation 2, main manuscript). Derivative of flux as a function of ***(a)*** *TMAC,* ***(b)*** *as a function of* α*, and* ***(c)*** *as a function of b. For flows with low TMAC (<0.1), derivative of flux is three orders of higher in comparison to dependence with* α *and b, indicative that TMAC is the dominating parameter in dictating mass transport.*

S6. Draw dilution as a function of varying draw osmotic (vapor) pressure

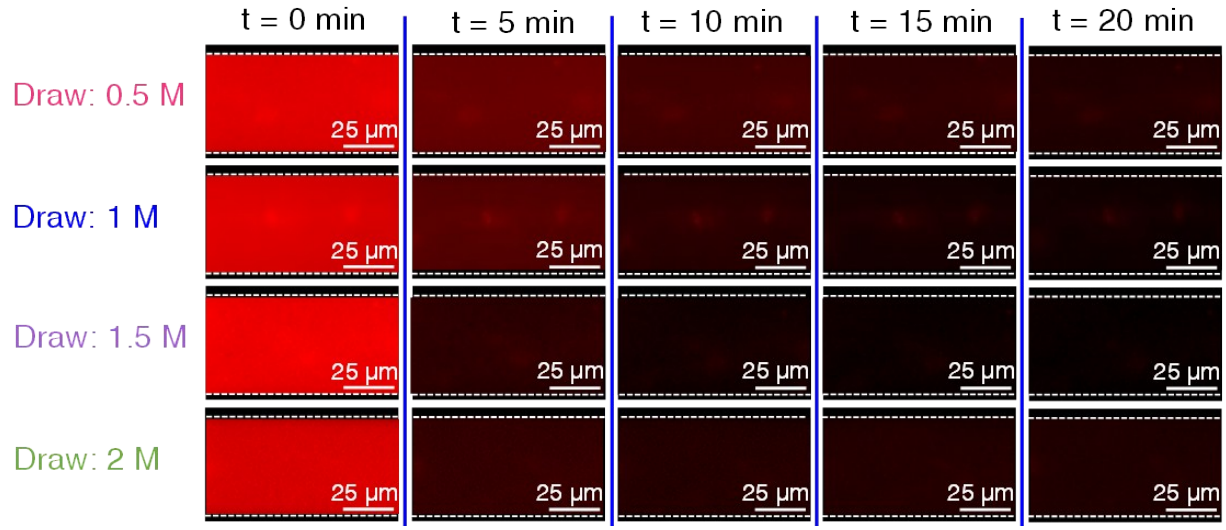

Figure S6: Images capturing reduction in Rhodamine B intensity at draw as a function of time for vapor-trap with varying osmotic gradients for FTS-modified channel with l_h = 96µm.

S7. Draw dilution in OTS-modified nanochannels

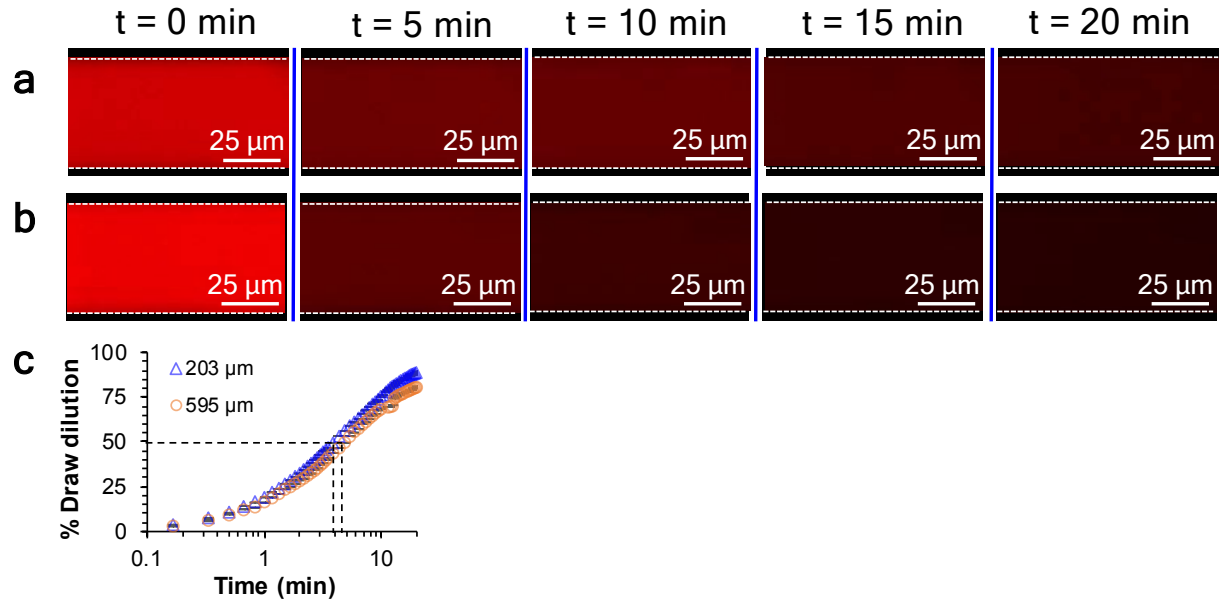

Figure S7: Fluorescence image showing desalting of 1 M NaCl tagged with 0.1 mM Rb dye in draw for OTS-modified nanochannels with ***(a)*** *l_h = 203 µm and* ***(b)*** *l_h = 595 µm.* ***(c)*** *Comparison of % draw dilution in channels with l_h = 203 µm and 595 µm, depicting the time necessary to achieve a 50% dilution is faster by only about ~1 min in channels with l_h = 203 µm despite a ~3x difference in length between the two cases.*

S8. Numerical model of convection-diffusion equation in microchannel

The governing equation used for convection-diffusion model in the draw microchannel

$$\frac{\partial \vec{u}}{\partial x} = 0$$

$$\frac{\partial c}{\partial t} - D_i \frac{\partial^2 c}{\partial x^2} + \vec{u}\frac{\partial c}{\partial x} = 0 \qquad \text{(S3)}$$

where D_i, is the diffusion coefficient of Rb dye in water (3.6 x 10^{-10} m^2s^{-1})[S10], c, instantaneous concentration of Rb, and $\vec{u}$ instantaneous velocity of condensing water in draw microchannel along x (Fig. 1a for coordinate system). Convection-diffusion equations were solved (in COMSOL) for the average velocity along *x-axis,* though the flow is fully developed in the transverse directions (along *y, z-axis*, Figure 1a). The diffusive flux competes to increase the draw intensity near the imaging region, whereas the convective flux of continuously condensing water reduces the dye intensity. Reduction in draw concentration over time due to dilution, reduces the local osmotic pressure, increasing the vapor pressure in the draw (Equation 1, in main manuscript) compared to t = 0. As a result, the net vapor pressure difference between feed and draw continue to decrease, reducing the flux in the draw i.e., $u(t) = \frac{u(t=0)\, c_{rb}(t)}{c_{rb}(t=0)}$

Boundary conditions include: (1) Draw concentration of Rb was 0.1 mM throughout draw at start of experiment, $c[0,x] = 0.1\,mM$; and (2) free-stream concentration of Rb away from the micro-channel nanochannel junction remains unvarying, and has a value of 0.1 mM.

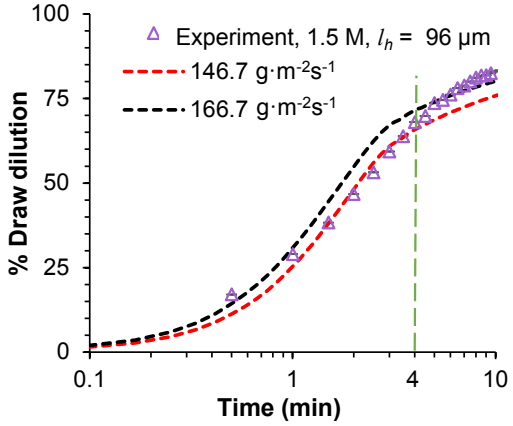

Figure S8: Numerically estimated dilution in draw compared against experimental dilution for a representative case of 1.5 M draw concentration, DI water feed and FTS-modified nanochannel with $l_h = 96$ µm. From the plot, higher J_{nano} (166.7 g·m^{-2}·s^{-1}) satisfies draw dilution rate at t > 4 min,

whereas a lower J_{nano} (144.7 $g \cdot m^{-2} \cdot s^{-1}$) satisfies draw dilution for t < 4 min. Therefore, the average of the two fluxes from the fit line was reported in Fig. 4a in the main manuscript.

Péclet Number Analysis: For the flux range reported in the manuscript for all tested cases (Figure 3, 4, main manuscript), the non-dimensional Péclet Number (*Pe*) was also estimated, where $Pe = ul/D$, u is the convective flux of water, l is the length of imaging region, and D is diffusion coefficient of Rb, (supporting information). *Pe* varies between 0.14 – 0.44 in the draw microchannel, implying equivalence in the contribution of the convective flux of water and the diffusive flux of Rhodamine B for all our tested cases. However, if transport were diffusion dominated, then $Pe << 1$, and no reduction in dye would be observed over the time scale of the experiment.

Supplementary information references

S1. E.W. Washburn, The Dynamics of Capillary Flow. *Phys. Rev.*, **1921**, *17*, 273-283.

S2. N. R. Tas; J. Haneveld; H. V. Jansen; M. Elwenspoek; A. v. d. Berg, Capillary Filling Speed of Water in Nanochannels. *Appl. Phys. Lett.*, **2004**, *85*, 3274-3276.

S3. A. Han, G. Mondin; N. G. Hegelbach; N. F. de Rooij; U. Staufer, Filling Kinetics of Liquids in Nanochannels as Narrow as 27 nm by Capillary Force. *J. Colloid Interface Sci.*, **2006**, *293*, 151-157.

S4. L. H. Thamdrup; F. Persson; H. Bruus; A. Kristensen; H. Flyvbjerg, Experimental Investigation of Bubble Formation During Capillary Filling of SiO_2 nanoslits. *Appl. Phys. Lett.*, **2007**, *91*, 163505.

S5. M. Yang; B.-Y. Cao; W. Wang; H.-M. Yun; B.-M. Chen, Experimental Study on Capillary Filling in Nanochannels. *Chemi.Phys. Lett.*, **2016**, *662*, 137-140.

S6. M. Fuest; C. Boone; K.K. Rangharajan; A.T. Conlisk; S. Prakash, A Three-State Nanofluidic Field Effect Switch. *Nano Lett.*, **2015**, *15*, 2365–2371.

S7. J. Lee; T. Laoui; R. Karnik, Nanofluidic transport governed by the liquid/vapour interface. *Nat. Nanotechnol.*, **2014**, *9*, 317-323.

S8. V. Teske; E. Vogel; Bich E. Viscosity Measurements on Water Vapor and Their Evaluation. *J. Chem. Eng. Data*, **2005**, *50*, 2082-2087.

S9. W.H. Fissell; A.T. Conlisk; S. Datta.; J.M. Magistrelli; J.T. Glass;A.J. Fleischman; S. Roy, High Knudsen number fluid flow at near-standard temperature and pressure conditions using precision nanochannels. *Microfluid. Nanofluid.*, **2011**, *10*, 425-433.

S10. S.A. Rani; B. Pitts; P.S. Stewart, Rapid Diffusion of Fluorescent Tracers into Staphylococcus epidermidis Biofilms Visualized by Time Lapse Microscopy. *Antimicrob. Agents Chemother.,* **2005**, *49*, 728-732.